# SYNTHESES AND STRUCTURES OF DONOR–ACCEPTOR COMPLEXES OF SELENIUM DIOXIDE WITH PYRIDINE AND TRIMETHYLAMINE

Jiří TOUŽÍN[a1,*], Kamila NEPLECHOVÁ[b], Zdirad ŽÁK[a2] and Miloš ČERNÍK[a3]

[a] *Department of Inorganic Chemistry, Masaryk University, 611 37 Brno, Czech Republic; e-mail: [1] touzin@chemi.muni.cz, [2] zak@chemi.muni.cz, [3] cernik@chemi.muni.cz*

[b] *Institute of Biophysics, Academy of Sciences of the Czech Republic, Královopolská 135, 612 65 Brno, Czech Republic; e-mail: kamila@ibp.cz*

Received December 14, 2001
Accepted April 8, 2002

Donor–acceptor (DA) complexes of pyridine (py)·$SeO_2$ and trimethylamine (TMA)·$SeO_2$ were prepared by direct reactions of solid selenium dioxide with the amines. Both are white solids decomposing slowly at room temperature. The former complex decomposes into its components, while the latter one undergoes a redox reaction. The single-crystal structure determination of py·$SeO_2$ has revealed that the chain-like structure of $(SeO_2)_n$ is destroyed during the formation of the DA bond and the py·$SeO_2$ molecule is bound to the nearest neighbouring molecule through two weak Se···O interactions. More labile TMA·$SeO_2$ complex could not be prepared as single crystals. Analogous molecular structure of both complexes was proved by their Raman spectra. A modified general valence force field was used for the interpretation of Raman spectra of TMA·$SeO_2$ and TMA·$SO_2$.

**Keywords**: DA complex; Selenium dioxide; Pyridine; Amines; Crystal structure; Raman spectra; Normal coordinate analysis; X-Ray diffraction.

Donor–acceptor complexes of sulfur dioxide with pyridine[1] and trimethylamine[2] of the general formula B·$SO_2$ (B = py, TMA) were prepared by direct reaction of the components. Complex py·$SO_2$ was characterised by Raman spectroscopy[3]; TMA·$SO_2$ complex, apart from electronic[4], vibrational[5,6] and microwave[7] spectra, was also studied by single-crystal X-ray analysis[8].

The reaction of selenium dioxide with pyridine has been studied in connection with its use as an oxidising agent in organic synthesis. Adducts of the types 2py·$SeO_2$ (ref.[9]), py·$SeO_2$ (ref.[10]) and py·2$SeO_2$ (ref.[11]) have been reported. None of them, however, was sufficiently characterised since in all the cases the aduct was not a chemical individuum. Mishiev *et al.*[10] characterised py·$SeO_2$ by $^1$H NMR spectroscopy ($CH_3OD$, multiplet, chemical shift δ 7.95–8.58 ppm, downfield shift 0.95 ppm relative to the free pyridine) and by IR spectroscopy (two bands at 1 370 and 1 200 $cm^{-1}$ that were misassigned to vibrations of the $SeO_2$ group)[10].

Analogous reaction with trimethylamine has not been studied so far. We, therefore, attempted to prepare donor–acceptor complexes of both bases with $SeO_2$ with the aim of gaining information on their composition, properties and structure.

## EXPERIMENTAL

Selenium dioxide was obtained by resublimation of a commercial product. Pyridine was refluxed with selenium dioxide, then distilled from barium oxide, boiled with phosphorus pentoxide and distilled. Trimethylamine was dried by passing over solid potassium hydroxide and sodium wire, purified by boiling with selenium dioxide and then distilled. Tetravalent selenium was determined iodometrically[12], pyridine by UV spectroscopy ($\lambda$ = 255 nm). Trimethylamine was displaced from the samples by 30% KOH and determined by the Kjeldahl method. Single-crystal diffraction data were collected at –150 °C on a KUMA KM-4 kappa axis diffractometer using MoK$\alpha$ radiation. The programs employed were SHELXS86 (ref.[13]) for the structure solutions and SHELXL93 (ref.[14]) for the refinement and geometry calculations; drawings were made using ORTEP (ref.[15]). Raman spectra (in $cm^{-1}$) were recorded on a SPEX Ramalog 3 spectrometer. The samples were excited by the 488 nm line of a Spectra Physics 165-03 $Ar^+$ laser (50–100 mW). Normal coordinate analysis was performed by the Wilson G,F-matrix method, using published programs[16].

### Preparation of py·$SeO_2$

Pyridine (28.14 g, 0.356 mol) was added to selenium dioxide (1.41 g, 0.013 mol) and the suspension heated in a closed system to 115–120 °C for 2 h to give a pale yellow solution. After decanting this solution from undissolved $(SeO_2)_n$ and reducing its volume to 50% in vacuum, a white crystalline solid was obtained. The product was filtered off and the remaining pyridine was evaporated in vacuum at 20 °C. Yield about 45%. Hygroscopic py·$SeO_2$ melts in sealed capillary at 54 °C with decomposition. For py·$SeO_2$ (190.1) calculated: 41.62% py, 41.54% $Se^{IV}$; found: 42.20% py, 40.72% $Se^{IV}$. Raman spectrum: 142 s, 166 s, 260 w, 302 vw, 370 w, 395 vw, 439 vw, 638 w, 647 w, 763 vw, 871 vs, 895 m, 1 017 m, 1 031 m, 1 064 vw, 1 156 vw, 1 196 w, 1 478 vw, 1 558 vw, 1 600 vw.

### Preparation of TMA·$SeO_2$

Liquid trimethylamine (5.07 g, 0.086 mol) of was condensed onto selenium dioxide (0.78 g, 7 mmol). The mixture was heated to 50 °C and then cooled to –50 °C. A white powder was obtained, from which TMA was removed in vacuum at –30 °C. The very labile substance was stored at low temperature. Yield about 70%. For TMA·$SeO_2$ (167.1) calculated: 33.58% TMA, 47.26% $Se^{IV}$; found: 33.71% TMA, 46.58% $Se^{IV}$. Raman spectrum: 141 s, 180 w sh, 232 vw sh, 284 vw, 313 vw, 376 w, 419 m, 435 m, 810 m, 829 vw, 866 vs, 874 m sh, 1 005 vw sh, 1 033 vw, 1 099 vw, 1 214 s, 1 396 vw, 1 432 w, 1 478 vw.

## RESULTS AND DISCUSSION

The solubility of pure selenium dioxide in anhydrous pyridine at laboratory temperature is very low, increasing very slowly when heating to the boiling point of pyridine. The solubility substantially increases when heating further in a closed system. At the same time, however, the amount of oily fluorescent side products, which cannot be quantitatively removed from the desired adduct, rises. The best method for preparation of pure py·$SeO_2$ was to set the reaction temperature slightly above the boiling point of pyridine. The py·$SeO_2$ adduct is also formed in the reaction of $Se_3O_7$ with pyridine[17] or by thermal decomposition of py·$Se^{IV}O(OSi(CH_3)_2)$ (ref.[18]). In both these cases, the reagents are hardly available. Hence, for preparative use the direct reaction of the components is the most suitable solution. When heated in an open system, py·$SeO_2$ starts to release pyridine already at 30 °C; the decomposition is complete at 180 °C.

### *Crystal Structure of py·$SeO_2$*

The structure of py·$SeO_2$ was solved by a heavy-atom method in a straightforward manner and refined anisotropically on $F^2$. Details of the structure determination are given in Table I. The structure consists of py·$SeO_2$ molecules joined into dimers (Fig. 1) through weak intermolecular Se···O contacts (2.996(4) Å), clearly shorter than the sum of the van der Waals radii of Se and O atoms (3.4 Å). Both pyridine rings are coplanar and include the angle 37.8° with the $Se_2O_2$ plane.

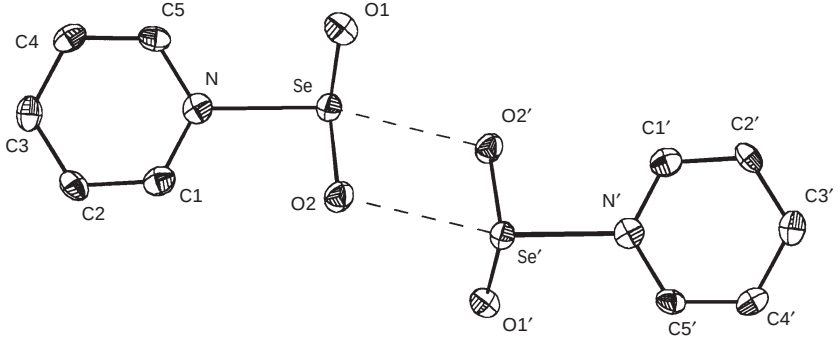


FIG. 1
ORTEP representation of the py·$SeO_2$ dimer (thermal ellipsoids drawn with 50% probability)

TABLE I
Experimental data for the X-ray diffraction study of py·$SeO_2$

| | |
|---|---|
| Empirical formula | $C_5H_5NO_2Se$ |
| $M_w$ | 190.06 |
| $T$, K | 120(2) |
| λ, Å | 0.71073 |
| Crystal system | monoclinic |
| Space group | $P2_1/n$ |
| $a$, Å | 7.673(6) |
| $b$, Å | 3.903(3) |
| $c$, Å | 20.43(2) |
| α, ° | 90 |
| β, ° | 93.69(8) |
| γ, ° | 90 |
| $V$, Å$^3$ | 610.6(9) |
| $Z$ | 4 |
| $D_c$, g cm$^{-3}$ | 2.068 |
| μ, mm$^{-1}$ | 6.063 |
| $F$(000) | 368 |
| Crystal size, mm | 0.50 × 0.15 × 0.10 |
| θ range of data collection, ° | 2.78–26.53 |
| Index ranges | $-9 \le h \le 9$, $-4 \le k \le 0$, $-25 \le l \le 17$ |
| No. of reflections measured | 1 620 |
| No. of independent reflections | 1 254 |
| $R_{int}$ | 0.0686 |
| Refinement method | Full-matrix least-squares on $F_o^2$ |
| Data, restraints, parameters | 1 244; 0; 82 |
| Goodness-of-fit on $F^2$ | 1.073 |
| $R_1$, $wR_2$[a], final [$I > 2\sigma(I)$] | 0.0428, 0.1119 |
| $R_1$, $wR_2$, all data | 0.0710, 0.1462 |
| Largest difference peak and hole, e Å$^{-3}$ | 0.841; –0.906 |

[a] $wR_2 = [\Sigma[w(F_o^2 - F_c^2)^2]/\Sigma w(F_o^2)^2]^{1/2}$, where $w^{-1} = [\sigma^2(F_o^2) + (aP)^2 + bP]$ and $P = [\max(F_o^2, 0) + 2F_c^2]/3$.

The molecular packing in the elemental cell is shown in Fig. 2. Important bond lengths and angles are given in Table II. The donor–acceptor bond Se–N (2.17 Å) is substantially longer than covalent bonds Se–N in nitrogen

TABLE II
Selected bond lengths (in Å) and angles (in °) for py·$SeO_2$

| | | | |
|---|---|---|---|
| Se–O2 | 1.652(4) | O2–Se–O1 | 110.4(2) |
| Se–O1 | 1.655(4) | O2–Se–O2[a] | 81.6(2) |
| Se–N | 2.171(4) | O1–Se–O2[a] | 105.4(2) |
| Se–O2 | 3.000(4) | N–Se–O2[a] | 158.53(13) |
| C1–N | 1.345(7) | N–C1–C2 | 121.1(4) |
| C1–C2 | 1.396(7) | C1–C2–C3 | 119.3(5) |
| C2–C3 | 1.397(7) | C2–C3–C4 | 119.0(5) |
| C3–C4 | 1.410(7) | C5–C4–C3 | 118.5(4) |
| C4–C5 | 1.403(7) | N–C5–C4 | 121.3(5) |
| C5–N | 1.344(6) | C5–N–C1 | 120.8(4) |
| O2–Se–N | 93.9(2) | C5–N–Se | 120.4(3) |
| O1–Se–N | 95.2(2) | C1–N–Se | 118.7(3) |

[a] Symmetry transformations used to generate equivalent atoms: #1 *–x*, *–y*, *–z*.

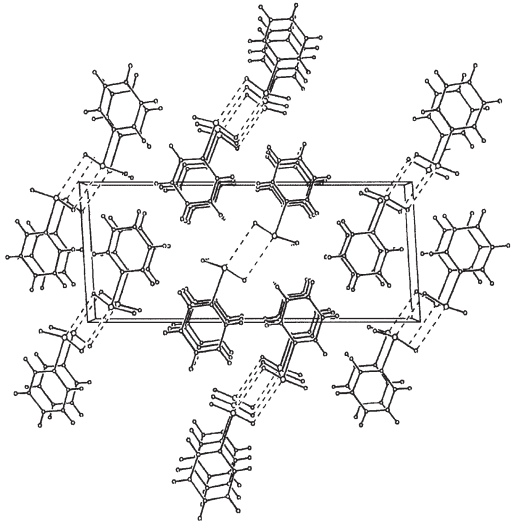

FIG. 2
Molecular packing of py·$SeO_2$ as viewed along the *b*-axis

derivatives of selenic acid[19] (1.77 to 1.82 Å) but comparable with the lengths of donor–acceptor bonds in 4py·$Se_2O_5$ (2.18–2.47 Å) (ref.[17]) and 2py·$SeOCl_2$ (2.19 Å) (ref.[20]).

CCDC 169736 contains the supplementary crystallographic data for this paper. These data can be obtained free of charge via www.ccdc.cam.ac.uk/conts/retrieving.html (or from the Cambridge Crystallographic Data Centre, 12, Union Road, Cambridge, CB2 1EZ, UK; fax: +44 1223 336033; or deposit@ccdc.cam.ac.uk).

*Raman Spectra and Normal Coordinate Analysis*

Raman spectra of both donor–acceptor complexes are depicted in Figs 3 and 4. The assignment of the bands due to stretching vibrations of the $SeO_2$ group in the region 800–900 $cm^{-1}$ is unambiguous in both spectra. In the case of py·$SeO_2$, no bands of the donor molecule lie in this range. For TMA·$SeO_2$ there can be observed a medium intense band due to the symmetrical stretching vibration $\nu_s(NC_3)$ (810 $cm^{-1}$) and a very weak band at 829 $cm^{-1}$ belonging to the same vibration of the free amine that could not be removed from the sample without its partial decomposition.

The character of both spectra in the region 500–800 $cm^{-1}$ confirms that no bridging bonds Se–O–Se are present in the adducts and that the linear polymer chains of selenium dioxide are cleaved to monomers by the attack of the base. In the spectrum of TMA·$SeO_2$, there is no band in this region; three weak bands at 638, 647 and 763 $cm^{-1}$ in the spectrum of py·$SeO_2$ be-

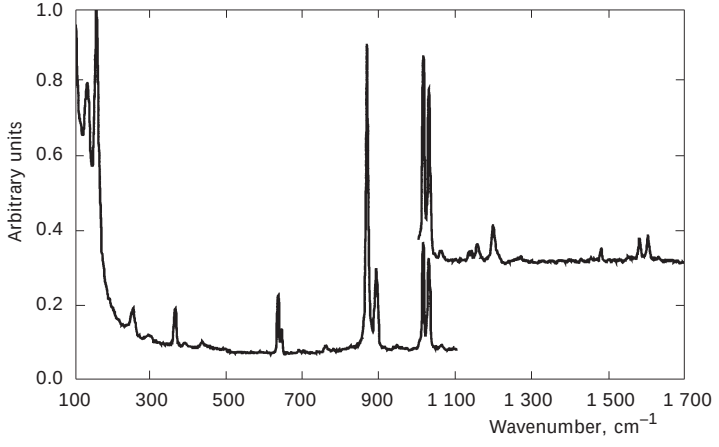


FIG. 3
Raman spectrum of py·$SeO_2$

long[21] to normal vibrations of pyridine $\nu_3$, $\nu_{12}$ and $\nu_{23}$. Weak intermolecular interactions Se–O···Se that were found in py·$SeO_2$ crystals, are not observed in this region. Comparison of the wavenumbers belonging to normal vibrations of pyridine in DA complex py·$SeO_2$ with those of free pyridine and its other DA complexes gives the possibility of estimating the strength of DA interaction in these compounds[22]. This criterion suggests that the strengths of the DA bonds in py·$SeO_2$ and py·$SO_2$ are approximately the same and much lower than those in the adducts of pyridine with sulfur trioxide and selenium trioxide[18].

Deformational vibrations in the N–$SeO_2$ group and stretching vibrations of the DA bond Se–N lie in the wavenumber region below 450 $cm^{-1}$. Non-characteristic vibrations in TMA·$SeO_2$ were interpreted with the aid of normal coordinate analysis. Simultaneously, the calculations were also performed for TMA·$SO_2$ in order to assess whether the assignment is consistent for both spectra. Fundamental frequencies for TMA·$SO_2$, except $\tau$(CNSO), were read out from the Raman spectrum of the solution in liquid $SO_2$ (ref.[6]), while for TMA·$SeO_2$ the wavenumbers from the Raman spectrum of a microcrystalline sample were used.

Molecules TMA·$ZO_2$ (Z = S, Se) with optimum mutual positions of donor and acceptor parts can belong at maximum to point group $C_s$. If, for simplification, the $CH_3$ groups are considered as vibrating units with relative weight of *ca* 15, they can exercise 15 normal vibrations. They are all active both in IR and Raman spectra and their division into symmetry types is described by fully reduced vibrational representation $\Gamma$ = 9 A′ + 6 A″. Out of

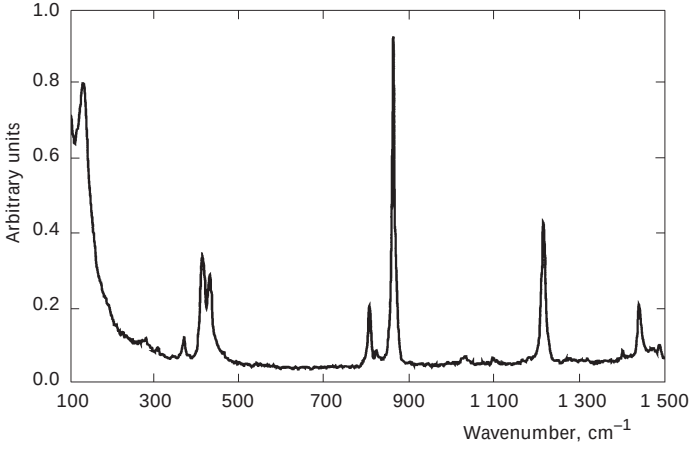


FIG. 4
Raman spectrum of TMA·$SeO_2$

nine vibrations of the type A′, four are stretching and five are deformational; of six vibrations of the type A″, two are stretching and four are deformational (see Table IV). Structural parameters of the TMA·$SO_2$ molecule were taken from[8]; for the N–$SeO_2$ group, the values determined for py·$SeO_2$ and the geometry of the $NC_3$ group were considered identical in both adducts. Details of the chosen set of internal symmetrical coordinates, modification of the general valence force field, and the procedure of calculation of quadratic potential constants are described in ref.[18]

Out of fifteen adjusted parameters, final values only for ten quadratic potential constants (QPC) are listed in Table III. The values $f_{ZN}$ are lower, and $f_{CN}$ slightly higher than for adducts TMA·$ZO_3$ (ref.[6]). This is in accordance with lower strength of DA interaction in adducts of oxides $ZO_2$, and with the associated change in polarity of C–N bonds. The last five parameters are the elements of ***F*** matrix ($F_{66}^{A'} = F_{33}^{A''}$, $F_{77}^{A'}$, $F_{99}^{A'} = F_{55}^{A''}$, $F_{29}^{A'}$ and $F_{57}^{A'}$), whose individual QPC constants cannot be calculated. By the re-insertion of all fifteen adjusted parameters in the secular equation, the experimental values of the fundamental frequencies are reproduced with an absolute error not exceeding 1 $cm^{-1}$.

Interpretation of Raman spectra of both studied donor–acceptor complexes of TMA, together with data on distribution of potential energy into

TABLE III
Quadratic potential constant (QPC, in N $m^{-1}$) of TMA·$ZO_2$ (Z = S, Se)

| QPC | TMA·$SO_2$ | TMA·$SeO_2$ |
|---|---|---|
| $f_{ZO}$ | 853.7 | 590.3 |
| $f'_{ZO}$ | –20.88 | 25.16 |
| $f_{CN}$ | 317.4 | 320.8 |
| $f'_{CN}$ | 25.32 | 23.07 |
| $f_{ZN}$ | 204.9 | 177.4 |
| $f_{OZO}$ | 90.81 | 53.99 |
| $f_{OZN}$ | 45.41 | 26.90 |
| $f'_{OZN}$ | –21.77 | –13.23 |
| $f_{OZNC}$ | 3.75 | 2.76 |
| $f_{ZN/OZN}$ | 23.09 | 22.07 |

individual symmetric coordinates, are listed in Table IV. It can be seen that all stretching vibrations of both adducts are fully characteristic, except vibrations of DA bonds, ν(ZN). They occur together with several deformational vibrations of groups $ZO_2$ and $NC_3$ in the wavenumber range 450–200 $cm^{-1}$ and are subjected to significant mixing that results in total loss of characteristics. As a result, a surprising dominance of ν(SeN) in the band at 419 $cm^{-1}$ arises, while the band with prevalent ν(SN) lies lower by *ca* 30 $cm^{-1}$. The ν(SN), however, does not considerably contribute to lower-positioned bands, while ν(SeN) significantly influences the origin of bands at 313 a 232 $cm^{-1}$.

TABLE IV
Fundamental IR modes of TMA·$ZO_2$ (Z = S, Se)

| No. | Assignment | TMA·$SO_2$ | | TMA·$SeO_2$ | |
|---|---|---|---|---|---|
| | | $\tilde{\nu}$, $cm^{-1}$ | PED[a], % | $\tilde{\nu}$, $cm^{-1}$ | PED[a], % |
| | | Type A′ | | | |
| 1 | $\nu_s(ZO_2)$ | 1 091 | $93\nu_1$ | 866 | $97\nu_1$ |
| 2 | $\nu'_s(NC_3)$ | 1 020 | $75\nu_2$ | 1 033 | $78\nu_2$ |
| 3 | $\nu_s(NC_3)$ | 796 | $72\nu_3$ | 810 | $74\nu_3$ |
| 4 | $\delta(ZO_2)$ | 555 | $76\nu_4$ | 376 | $98\nu_4$ |
| 5 | ν(ZN) | 386 | $59\nu_5 + 31\nu_8$ | 419 | $40\nu_5 + 33\nu_8$ |
| 6 | $\delta'_s(NC_3)$ | 435 | $57\nu_6 + 25\nu_7$ | 435 | $63\nu_6$ |
| 7 | $\omega(ZO_2)$ | 455 | $42\nu_7 + 23\nu_6$ | 313 | $73\nu_7 + 31\nu_5$ |
| 8 | $\delta_s(NC_3)$ | 297 | $69\nu_8 + 23\nu_7$ | 232 | $64\nu_8 + 31\nu_5$ |
| 9 | $\rho(NC_3)$ | 203 | $85\nu_9$ | 180 | $83\nu_9$ |
| | | Type A″ | | | |
| 10 | $\nu_{as}(ZO_2)$ | 1 274 | $97\nu_{10}$ | 874 | $99\nu_{10}$ |
| 11 | $\nu_{as}(NC_3)$ | 1 020 | $71\nu_{11}$ | 1 005 | $77\nu_{11}$ |
| 12 | $\delta_{as}(NC_3)$ | 455 | $58\nu_{12} + 27\nu_{11}$ | 435 | $77\nu_{12} + 20\nu_{11}$ |
| 13 | $\rho(ZO_2)$ | 386 | $69\nu_{13} + 23\nu_{12}$ | 284 | $77\nu_{13}$ |
| 14 | $\rho'(NC_3)$ | 203 | $89\nu_{14}$ | 181 | $81\nu_{14}$ |
| 15 | τ(CNZO) | 168 | $96\nu_{15}$ | 141 | $96\nu_{15}$ |

[a] Only contributions higher than 20% (rounded to integers) are given for potential energy distribution (PED).

**REFERENCES**


1. Hoffmann K. R., van der Werf C. A.: *J. Am. Chem. Soc.* **1946**, *68*, 997.
2. Burg A. B.: *J. Am. Chem. Soc.* **1943**, *65*, 1629.
3. a) Tramer A.: *Bull. Acad. Pol. Sci. C.III* **1956**, *4*, 355; b) Tramer A.: *Bull. Acad. Pol. Sci. C.III* **1957**, *5*, 501; c) Tramer A.: *Bull. Acad. Pol. Sci. C.III* **1957**, *5*, 509; d) Toužín J.: *Ph.D. Thesis*. Masaryk University, Brno 1974.
4. a) Moede J. A., Curran C.: *J. Am. Chem. Soc.* **1949**, *71*, 852; b) Christian S. D., Grundes J.: *Nature* **1967**, *214*, 1111; c) Grundes J., Christian S. D.: *J. Am. Chem. Soc.* **1968**, *90*, 2239.
5. Hata T., Kinumaki S.: *Nature* **1964**, *203*, 1378.
6. Toužín J., Bauer P.: *Collect. Czech. Chem. Commun.* **1981**, *46*, 2600.
7. Jung J. O., LaBarge M. S., Matos J., Kampf J. W., Hillig K. W., Kuczkowski R. L.: *J. Am. Chem. Soc.* **1991**, *113*, 4732.
8. van der Helm D., Childs J. D., Christian S. D.: *J. Chem. Soc., Chem. Commun. D* **1969**, 887.
9. Edgington B., Firth J. B.: *J. Soc. Chem. Ind., Trans. Commun.* **1936**, *55*, 198.
10. Mishiev R. D., Ibragimova D. S., Rzaeva Z. I., Mamedov E. Sh.: *Zh. Org. Khim.* **1992**, *28*, 2215.
11. Jerchel D., Bauer E., Hipchen H.: *Chem. Ber.* **1955**, *88*, 156.
12. Blanka B., Hudec P., Mošna P., Toužín J.: *Collect. Czech. Chem. Commun.* **1963**, *28*, 3434.
13. Sheldrick G. M.: *Acta Crystallogr., Sect. A: Fundam. Crystallogr.* **1983**, *39*, 876.
14. Sheldrick G. M.: *Acta Crystallogr., Sect. A: Fundam. Crystallogr.* **1990**, *46*, 467.
15. Johnson C. K.: *ORTEP II, Report ORNL-5138*. Oak Ridge National Laboratory, Tennessee 1976.
16. a) Špirko V., Klíma P., Hájek B.: *Sb. Vys. Sk. Chem.-Technol. Praze, Anorg. Chem., Chem. Technol. B* **1972**, *15*, 15; b) Adámek P., Hájek B.: *Sb. Vys. Sk. Chem.-Technol. Praze, Anorg. Chem., Chem. Technol. B* **1974**, *18*, 69.
17. Neplechová K., Žák Z., Toužín J.: *Main Group Chem.* **1997**, *2*, 149.
18. Neplechová K.: *Ph.D. Thesis*. Masaryk University, Brno 1996.
19. a) Žák Z., Růžička A., Glowiak T.: *Can. J. Chem.* **1991**, *69*, 1080; b) Žák Z., Růžička A.: *Acta Crystallogr., Sect. C: Cryst. Struct. Commun.* **1992**, *48*, 2254; c) Žák Z., Marek J., Keznikl L.: *Z. Anorg. Allg. Chem.* **1996**, *622*, 1101; d) Žák Z., Keznikl L.: *Z. Kristallogr.* **1996**, *211*, 544.
20. Lindquist I., Nahringbauer G.: *Acta Crystallogr., Sect. C: Cryst. Struct. Commun.* **1959**, *12*, 638.
21. Long D. A., Murfin D. S., Thomas E. L.: *Trans. Faraday Soc.* **1963**, *59*, 12.
22. Kurze R., Paetzold R.: *Z. Anorg. Allg. Chem.* **1972**, *387*, 367.